

Measuring height of reflection at HF

Sky-wave propagation at HF relies on radio waves refracted, bent downward, back to Earth. Refraction results in a curved path within the ionosphere, but a convenient simplification is to treat the path as a reflection with a sharp apex known as the virtual height [1].

Introduction

While the terms 'regions' and 'layers' are often used interchangeably, here I'll refer to the E and F regions, and F1 and F2 layers within the F region [2]. Virtual height, together with the operating frequency, and the reflecting region or layer's critical frequency, are key factors affecting minimum and maximum one-hop distances. Height of reflection varies with the time of day, the season, and the phase of the 11-year solar cycle. Changes in height are well illustrated by a diagram in the *Radio Communication Handbook's* Propagation chapter [1], reproduced here in **Figure 1**. These depictions represent the climate of the ionosphere, that is, they are typical of long-term behaviour. Actual day-by-day or hour-by-hour changes may be somewhat different. Consequently, the height of reflection is one of many variables constituting 'space weather'.

For ground-based routine measurements of heights, the professional instrument is the 'ionosonde'. Every 5 to 15 minutes, instruments within a global network of these specialised HF radars, typically sweeping from 1MHz to 25MHz, measure heights immediately overhead. Ionosondes have three major limitations: the measurements are for one location, are only for overhead at that location, and the global network is sparse. 37 ionosondes reported data on 20 May 2024 to the Global Ionosphere Radio Observatory (GIRO). The UK Chilton ionosonde had not reported data to the GIRO for the previous 34 days, but its latest ionogram may be available [3].

In contrast to this dwindling ground-based measurement capacity, there is growing interest in space-weather measurements by the amateur-radio and citizen-science communities. One example is the 'personal space weather station' initiative from HamSCI [4]. Their 'Grape' project, comprising software-defined radios (SDRs) and a data acquisition and reporting system, has been designed specifically to observe changes in the ionosphere. Over 30 stations in North America are involved, measuring the Doppler shift and signal level of standard frequency transmitters WWV, WWVH and CHU. An eighteen-author scientific paper on their early results illustrates substantial collaboration between professional scientists and the amateur-radio community [5].

This article shows how readily-available items, SDRs, and low-cost precision GPS-disciplined oscillators (GPSDO), with WSPR or FST4W digital communications protocols from WSJT-X, can be used to measure variations in reflection height. The morning descent of the F2 layer, and the change in height induced by the October 2023 annular eclipse over North America, are shown as worked examples.

Vertical vs oblique measurements

An ionosonde measures the virtual height h of regions and layers from the time delay of echoes:

$$h = ct/2,$$

where c is the speed of light and t the echo time delay for returns from the E and F regions and F1 and F2 layers. Reduced c in the ionosphere, a plasma, is accounted for in the electron density profile.

In contrast, height observations on an oblique path by amateurs, at least currently, measure path length change which results in a Doppler shift, rather than the absolute time of travel. We do have to assume a negligible change in ionospheric electron density as this affects the

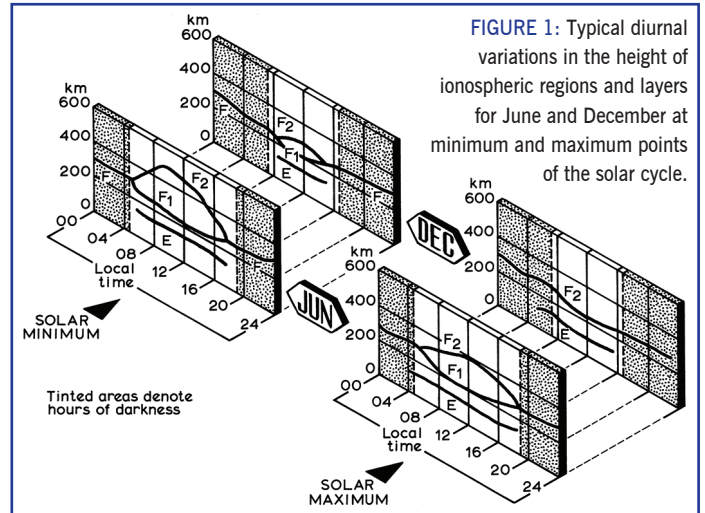


FIGURE 1: Typical diurnal variations in the height of ionospheric regions and layers for June and December at minimum and maximum points of the solar cycle.

speed of light. This is normally a safe assumption, but not during extreme events such as sudden ionospheric disturbances caused by solar flares [6]. Changes in reflection height can be inferred using simple geometry, while absolute height can be found by adding a constant of integration. This constant could come from an ionosonde once a day. An enticing feature of the oblique path method is that multiple measurements at multiple frequencies can be made over extensive areas from one transmitter and multiple receivers.

Measuring Doppler shift

Figure 2 shows the variation of Doppler shift at 7.04MHz on a 1,310km path from G3ZIL, Southampton UK, to Gerhard, OE3GBB, eastern Austria, with time of day and day of year from mid-winter to mid summer. Many aspects of propagation can be seen, but it is the positive Doppler shift in the morning as reflection height descends, and the negative Doppler shift in the evening as reflection height ascends, that concern us here. Immediately clear is that our measurements must be both stable, and accurate, to much better than 1Hz.

The block diagram in **Figure 3** shows the equipment used to gather the Doppler data of **Figure 2**. The gold standard for stability and accuracy is the GPSDO. Both the QRP Labs QDX digital-modes transceiver, and the KiwiSDR receiver, have had hardware and software modifications made by their manufacturers to improve frequency accuracy and stability, and to make it easier to use external clocks.

WsprDaemon software from Rob Robinett, AI6VN, enables simultaneous multi-band recording and reporting of WSPR and FST4W spots from KiwiSDRs (8 or 14 bands), or RX888 Mk II receivers running Phil Karn's ka9q-radio (15 WSPR/FST4W bands and 10 standard time bands simultaneously) [7]. While wsprnet.org only reports frequencies with 1Hz resolution, WsprDaemon reports with 0.1Hz, just adequate for this study.

Doppler variation: daily pattern

Measuring Doppler shift is the first step in finding reflection height. **Figure 4** shows the Doppler shift for simultaneous FST4W-120 transmissions on the 3.5MHz, 7MHz and 10MHz bands from Tom, WO7I, to Dennis, ND7M, both in Nevada, spanning 14-15 October 2023. First, we'll look at the Doppler shift around sunrise. The 3.5MHz frequency had been open during the night on this 545km

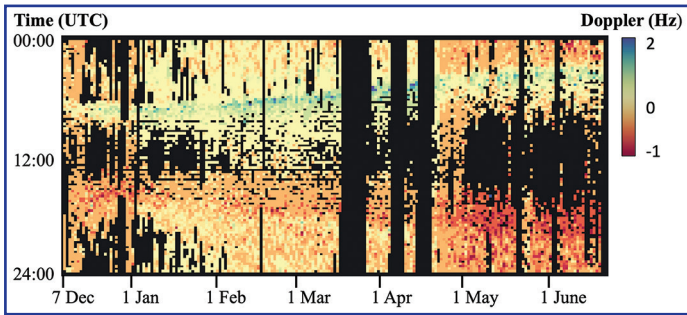


FIGURE 2: Doppler shift averaged over 15-minute intervals for 7.04MHz FST4W-120 transmissions from G3ZIL to OE3GBB over a 1310km path from December 2023 to June 2024. Black regions with no data were times of no propagation or when G3ZIL was not transmitting.

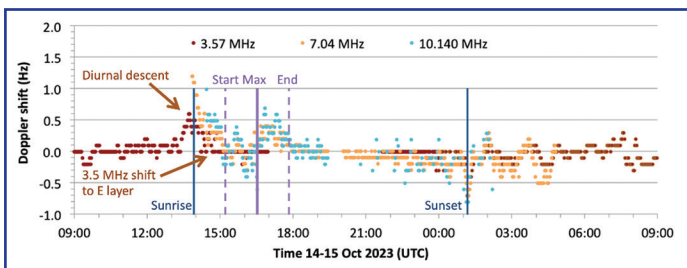


FIGURE 4: Doppler shift on the 545km path from WO7I to ND7M, both in Nevada, showing the diurnal pattern at 3.5MHz, 7MHz and 10MHz, and the effect of the annular eclipse of 14 October 2023.

path. Doppler shift started to increase before sunrise at ground level, sunrise occurring earlier at the height of the ionosphere, reaching a maximum of 0.6Hz. The refracting F2 layer was descending, reducing the path length, and producing a positive Doppler shift. As the layer descent slowed, the Doppler shift reduced, reaching zero at 1424UTC just over an hour after it had started to rise.

The 7MHz frequency opened too late to capture the initial descent, but showed a 1.2Hz Doppler shift around the time of most rapid descent. The 10MHz frequency opened later still, but captured the later part of the F2 layer's descent.

The positive Doppler shift at 7MHz and 10MHz showed the descent of the F2 layer continuing after 1424UTC, yet the 3.5MHz Doppler shift was zero. Why the difference? These results suggest that dominant propagation at 3.5MHz shifted from the descending F2 layer to the E region, which, as in the handbooks (eg Figure 1) hardly changes height.

The 3.5MHz frequency opened before sunset, initially via E-region propagation with low Doppler shift, but by sunset all three bands were showing a negative Doppler shift from the path length increasing, ie the F2-layer reflection height rising. The initial rise was followed by at least two sinusoidal cycles with a period of about 100 minutes. These were probably caused by travelling ionospheric disturbances, fascinating features affecting propagation that have been studied by ionospheric physicists using amateur radio techniques [8].

The rate of change of the path length

Focusing on the morning descent, the second step in finding reflection height is to convert Doppler shift, δf in Hz, to rate of change of path length, δP in metres per second:

$$\delta P = -c \delta f / f ,$$

where f is the operating frequency. Dividing by the operating frequency collapses the frequency-dependent Doppler shifts in Figure 4 onto the same pattern of path rate-of-change, irrespective of frequency, Figure 5.

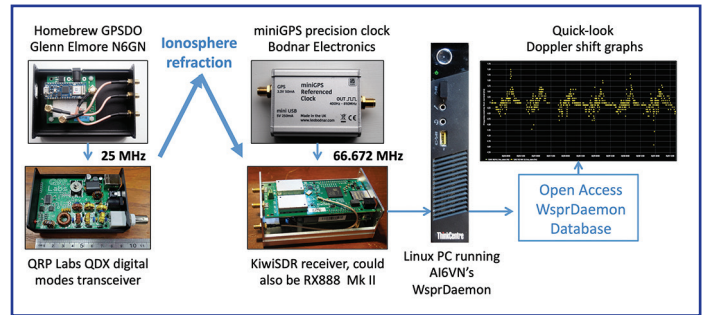


FIGURE 3: A block diagram, showing examples of general-purpose items needed to make routine simultaneous multi-band measurements of Doppler shift and signal level on the HF bands and of time-standard stations.

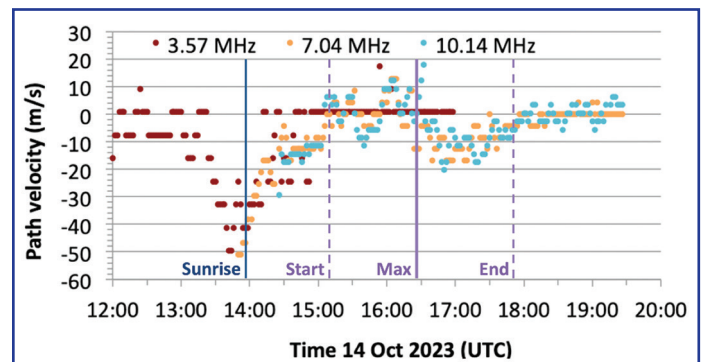


FIGURE 5: After converting Doppler shift to rate of change of path length, the measurements at three frequencies coalesced. The exception was when the 3.5MHz path reflected from the E region.

Reflection height

This is the trickiest step, requiring simplification, trigonometry, and a single measured overhead height from an ionosonde. Figure 6 shows the simplified geometry for a one-hop path. Reflection is shown as a sharp apex to the path at I . We know the distance, d , between WO7I and ND7M, 545km, and R , the radius of the earth, taken as 6371km. The angle θ (in radians) is given by

$$\theta = d / 2R .$$

Transmission path length, P , is the distance TX -> I -> Rx, which we do not know; we only know how rapidly the path changed. However, if we knew the reflection height, h , at one time, t_0 we can calculate path length at that time, P_0 , from the equation:

$$P_0 = 2\sqrt{(R\sin(\theta))^2 + (h+R(1-\cos(\theta)))^2} .$$

For the initial height, it was convenient to take the average of the minimum virtual height (227km) and the peak height (247km) of the F2 layer at 1445UTC from the ionosonde at Point Arguello, 570km SW of the midpoint between ND7M and WO7I [3].

Our WSPR and FST4W measurements are 120s apart. After two minutes, the path length, P_t , would become

$$P_t = P_0 + 120\delta P ,$$

which is simply the path velocity multiplied by the time interval, added to the initial distance. We then rearrange the equation for P_0 to estimate the reflection height, h_t , at time t , as follows:

$$h_t = \frac{1}{2}\sqrt{P_t^2 - (2R\sin(\theta))^2} - R(1-\cos(\theta)) .$$

Gwyn Griffiths, G3ZIL
gxgriffiths@virginmedia.com

After repeating the summation and height calculation for each successive two-minute interval, we have a time series of reflection heights, **Figure 7**. The blue vertical line at 1445UTC shows when we took the 237km reference height from the Point Arguello ionosonde. The 3.5MHz data usefully covered the 100km descent from 325km to 225km. As the 7MHz path, then 10MHz, opened they traced a similar descent. During descent, the inferred virtual height at all three frequencies lay just below hmF2, the height of the F2 layer peak electron density, rather than its minimum virtual height h'F2. After 1700UTC the picture changed: the reflection heights followed h'F2.

Effects of the annular eclipse

Magenta lines on Figures 4 and 5 show the times of the start of the eclipse, maximum obscuration (91%), and end. While small, at no more than 0.7Hz, there was a clear, consistent, pattern to the Doppler shift at 7MHz and 10MHz. After conversion to path velocity, Figure 5, while there was some scatter, both frequencies showed approximately the same path velocity pattern during the eclipse.

Figure 8 shows the reflection height centred on the time of maximum obscuration. Also shown is the average reflection height from the same equipment the following day. The disturbance caused by the eclipse stands out. As the eclipse started, diurnal descent was held in check: the effect of the rising Sun appeared to be balanced by the dimming effect of the eclipse. From halfway between the start and the point of maximum obscuration, the dimming more than countered the rising Sun: the F2 layer rose, as it does each evening. After maximum obscuration, the reflection height descended, ending close to its value measured the following day. The maximum height change was 30-35km.

To verify these results from FST4W transmissions, the magenta trace in Figure 8 shows the same analysis applied to continuous Doppler-shift measurements of WWV's 10MHz signal received by the HamSCI Grape receiver at St. George, Utah, an 830km path with its midpoint 680km east of the WO7I to ND7M midpoint. The difference between reflection height measured by the two systems at the eclipse maximum was only 2 km, and the later peak on the WWV to St George path was mostly because maximum obscuration was seven minutes later.

End note

Studies of changes in the height of ionospheric reflection can now be made with easily available receivers and transmitters using the WSPR or FST4W modes. The necessary precision does require GPS-disciplined oscillators, but these are readily available and affordable items. The data reporting path via

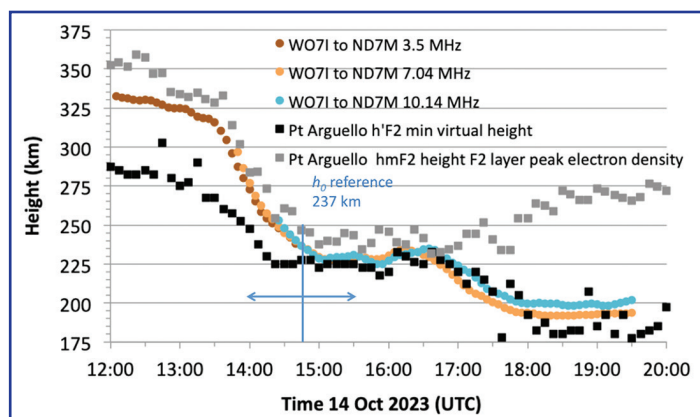


FIGURE 7: Reflection heights at three frequencies on the 545km path from WO7I to ND7M, calculated from the observed Doppler shift and a single reference height from the Point Arguello ionosonde at 1445UTC on 14 October 2023. Also shown are the F2 layer minimum virtual height, and peak electron density height, as reported by the ionosonde.

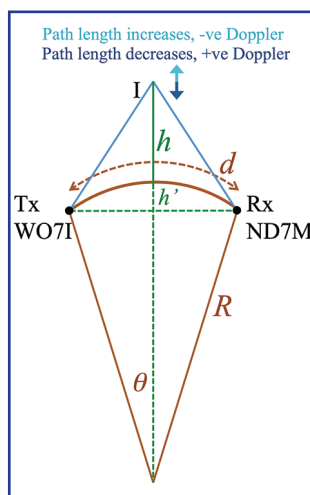


FIGURE 6: Simplified geometry for a one-hop path to convert from path length to reflection height.

WsprDaemon is well proven and, as we've seen, the mathematics to go from measured Doppler shift to reflection height is straightforward. It has never been easier for a radio amateur to study this fascinating aspect of space weather.

Acknowledgment

I am grateful to Rob Robinett, AI6VN, for WsprDaemon and the WSJT-X development team for FST4W.

Specific data for this article came from Tom Bunch, WO7I, using the WsprSonde transmitter from Paul Elliot, WB6XCX, and the receivers of Dennis Benischek, ND7M, Lee Phebus, KF7YRS, and Gerhard Burian, OE3GBB. Ionosonde data from Point Arguello via GIRO was released under CC-BY-NC-SA 4.0 license, with gratitude to the Point Arguello team.

References

- [1] Radio Communication Handbook, 2020. M. Browne (editor), RSGB, pp 12.15, 12.12
- [2] <https://www.ngdc.noaa.gov/stp/IONO/ionostru.html>
- [3] Global Ionosphere Radio Observatory ionosonde database at <https://giro.uml.edu/dibase/>. The latest Chilton ionogram may be available at https://www.ukssdc.ac.uk/cgi-bin/digsondes/latest_view2gif.pl?Station=chilton (registration needed)
- [4] <https://www.hamsci.org/basic-project/personal-space-weather-station>
- [5] Collins, K. et al., 2023. Crowdsourced Doppler measurements of time standard stations demonstrating ionospheric variability. *Earth System Science Data Discussions*, 15(3): 1403-1418. Available at <https://essd.copernicus.org/articles/15/1403/2023/>
- [6] Chum, J. et al., 2018. Continuous Doppler sounding of the ionosphere during solar flares. *Earth, Planets and Space*, 70, pp.1-19. Available at <https://earth-planets-space.springeropen.com/articles/10.1186/s40623-018-0976-4>
- [7] WsprDaemon software at <https://github.com/rrobinett/wsprdaemon>, with detailed information at <http://wsprdaemon.org/>, details of ka9q-radio at <https://github.com/ka9q/ka9q-radio>
- [8] Frissell, N.A. et al., 2022. First observations of large scale traveling ionospheric disturbances using automated amateur radio receiving networks. *Geophysical Research Letters*, 49(5), p.e2022GL097879. Available at <https://agupubs.onlinelibrary.wiley.com/doi/full/10.1029/2022GL097879>

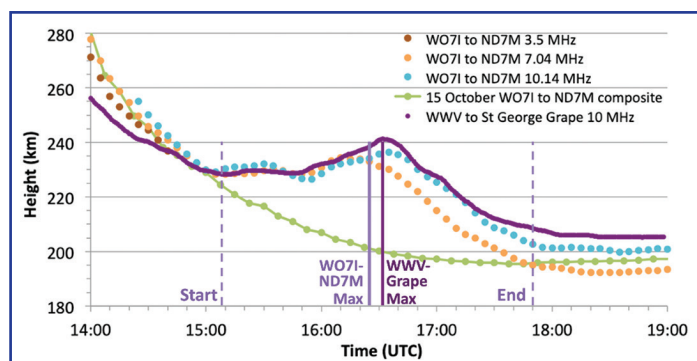


FIGURE 8: FST4W Doppler-derived reflection heights during the 14 October 2023 eclipse on the 545km path from WO7I to ND7M, and on the 830km path from continuous Doppler measurements of WWV 10MHz to the Grape receiver at St George, Utah. Comparison with the computed height for 15 October shows the effect of the eclipse in raising the height of reflection.